

## WHERE ARE THE HIGH VELOCITY CLOUDS?

VICENT QUILIS AND BEN MOORE

Physics Department, University of Durham, Durham DH1 3LE, UK

*Draft version November 18, 2018*

### ABSTRACT

Recent observations of high velocity clouds (HVCs) have revealed compression fronts and tail shaped features of HI suggesting that they are interacting with an external medium. We perform 3-D hydrodynamical simulations of HVCs moving through a diffuse hot gaseous component, investigating the behaviour of both extra-galactic dark matter dominated HVCs and nearby pure gas clouds that may be accreting onto the Galactic disk via a Galactic fountain. Both scenarios can give rise to similar features as observed if the external medium has a density  $> 10^{-4} \text{ cm}^{-3}$ . Observations suggest that this may be too high for a hot ionised halo or intergalactic gas and supports the Galactic fountain origin, a model that can also account for the high fraction of HVCs with tails and asymmetrical morphologies.

*Subject headings:* dark matter — galaxies: halos — galaxies: formation — galaxies: evolution

#### 1. INTRODUCTION

The nature of the high-velocity clouds (HVCs) seen in 21 cm HI emission remains controversial since their discovery over three decades ago (Muller, Oort & Raimond 1963). Most fundamentally, the distances, hence mass and environment of these objects remain poorly constrained, largely due to the difficulty of finding background sources (against which the clouds would appear in absorption) at known, comparable distances. It is possible that the HVCs may not have a single common origin, but rather they are a mix of relatively nearby ( $|z| < 10 \text{ kpc}$ ), “Galactic fountain” clouds, of material stripped from the Magellanic Clouds and other satellites of the Milky Way, and perhaps of extra-galactic objects (Blitz et al. 1999; Braun & Burton 1999, 2000). This latter possibility is most intriguing since the HVCs would provide a link to the numerous dark matter substructure halos expected in the hierarchical cold dark matter model (Moore et al. 1999, Klypin et al. 1999).

Previous studies have used the morphological, two phase core-envelope structure of the HVCs to infer approximate distances (Wolfire et al. 1995). Bland-Hawthorn & Maloney (1999) have proposed the use of sensitive  $H_\alpha$  emission measurements, together with a model for the ionizing photon flux as a function of position within the Galactic halo to infer their distances. A handful of HVCs have upper distance limits that are  $\lesssim 10 \text{ kpc}$  due to the presence of background stars (c.f. Gibson et al. 2000).

Brüns et al. (2000, 2001) found that  $\approx 20\%$  of HVCs exhibit position-velocity gradients, termed *head-tail* HVCs by analogy with the structures of comets. A likely cause for their elongated morphology is that they are interacting with a more diffuse, ionized ambient wind. Further evidence for such cloud-halo interactions are evident from the compressed leading fronts of many HVCs. In this letter we use high resolution hydro-dynamical simulations to examine the morphologies of HVCs moving through a diffuse medium. This allows us to infer the efficiency of the stripping process and will place limits on the possible environment of the HVCs. A detailed study of the interaction between clouds and a diffuse medium can be found in Murray et al. (1993).

#### 2. THE STRUCTURE OF THE HVCS

The typical angular size of HVCs are  $\theta \sim 1^\circ$  and in order to be included in existing catalogues (eg, Brüns et al. 2000) their HI column density,  $N_{HI}$ , should be  $\gtrsim 10^{19} \text{ cm}^{-2}$ . For a cloud at distance  $D$ , we can estimate its radius,  $R$ , mean spatial HI density,  $n_c$ , and mass,  $M_c$ , as follows.  $R = \theta D \sim 2 \text{ kpc}(\theta/1^\circ)(D/100 \text{ kpc})$  and  $n_c = N_{HI}/2R$ , i.e.

$$n_c \simeq 10^{-3} \text{ cm}^{-3} \left( \frac{N_{HI}}{10^{19} \text{ cm}^{-2}} \right) \left( \frac{\theta}{1^\circ} \right)^{-1} \left( \frac{D}{100 \text{ kpc}} \right)^{-1}$$

The cloud mass  $M_c \simeq f_{HI}^{-1} N_{HI} \pi R^2 m_{HI}$ , can be written;

$$M_c \simeq 2 \times 10^5 f_{HI}^{-1} M_\odot \left( \frac{N_{HI}}{10^{19} \text{ cm}^{-2}} \right) \left( \frac{\theta}{1^\circ} \right)^2 \left( \frac{D}{100 \text{ kpc}} \right)^2$$

where  $f_{HI}$  is the neutral hydrogen fraction. A cloud is gravitationally bound when it satisfies the virial relation  $R\sigma_c^2 \simeq GM_c$ . With our model assumptions and  $\sigma_c \sim 10 \text{ km/s}$ , this translates to

$$10^{12} \frac{\text{cm}^2}{\text{s}^2} = 2 \times 10^{10} \frac{\text{cm}^2}{f_{HI} \text{ s}^2} \left( \frac{N_{HI}}{10^{19} \text{ cm}^{-2}} \right) \left( \frac{\theta}{1^\circ} \right) \left( \frac{D}{100 \text{ kpc}} \right)$$

The general conclusion is that the nearby HVCs at distances  $D = 1 - 10 \text{ kpc}$ , have masses  $M_c = 10 - 100 M_\odot$  and must be in pressure equilibrium with the warm ionised medium located within and above the galactic disk. HVCs at several hundred kpc may also be pressure confined by some external medium, or they may be gravitationally bound by a dark matter halo. For both type of clouds we assume that they consist mainly of warm gas with temperature  $T_c \sim 10^4 \text{ K}$ , velocity dispersion  $\sigma_c \sim 10 \text{ km/s}$ , and density  $n_c$ . The dark matter dominated HVCs are constructed by adopting a dark matter density profile  $\rho(r) = A/(r_c^2 + r^2)$  where  $A = v_{cir}^2/4\pi G$ ,  $v_{cir} = 15 \text{ km/s}$  and  $r_c = 1 \text{ kpc}$ . The HI lies primarily within the constant density core of the dark matter halo and we adjust its temperature profile to maintain hydro-static equilibrium.

A typical cloud may be at a distance of 300 kpc, have a radius of  $\approx 1$  kpc and a total gas mass of  $1.6 \times 10^7 M_\odot$ . This leads to a central column density of  $10^{20} \text{ cm}^{-2}$  which is higher than the average quoted by Wakker and van Woerden (1991) but similar to those observed by Brüns et al. (2001).

The diffuse halo material (number density  $n_w$ ) is taken to be at a temperature  $T_h \sim 10^6 \text{ K}$ , comparable to the virial temperature for a circular velocity of 200 km/s. The wind velocity  $v_w$  should be of this same order; this is confirmed by the observed distribution of HVC galactocentric velocities. Clouds ejected from the disk in a Galactic fountain would fall back to the disk with a velocity  $\approx \sqrt{GM_{\text{disk}}/z} \sim 200 \text{ km/s}$ , where  $M_{\text{disk}} \approx 5 \times 10^{10} M_\odot$  and vertical height  $z \approx 10$  kpc.

### 3. THE DENSITY OF DIFFUSE GAS IN GALACTIC HALOS

The properties of the diffuse outer halo of the Milky Way is poorly known. Such a halo is expected to exist as left over material that has been unable to cool since the formation of the Milky Way. Observations so far provide only upper limits on its mean density. Constraints come from the measured soft X-ray background (Snowden et al. 1997, Benson et al. 2000), from the dispersion measures of pulsars in globular clusters and in the Magellanic Clouds, from the kinematics (Moore & Davis 1994) or lifetime (Murali 2000) of the Magellanic Stream. All of these constraints place the density of the ionised Galactic halo gas  $n_w(50 \text{ kpc}) \lesssim 5 \times 10^{-5} \text{ cm}^{-3}$ . Blitz & Robishaw (2000) derive a halo gas density that is a factor of 2 lower than this at a distance of 200 kpc by applying ram pressure stripping to the halo dwarf spheroidals. Deep ROSAT observations of nearby disk galaxies provide complimentary upper limits on a very extended component, but they give positive detections of ionised gas close to the disks that has a density of  $n_w(10 \text{ kpc}) \approx 10^{-3} \text{ cm}^{-3}$  (Bregman & Houck 1997, Ehle et al. 1998). We caution that direct observational limits of the diffuse gas density at 200-500 kpc do not exist.

The fact that the HVCs are moving at 150-300 km/s through this medium provides an upper limit to its density by considering their terminal velocity (c.f. Benjamin & Danly 1997). The equation of motion of a pure gas cloud of mass  $m_c$ , area  $A$  and velocity  $v_c$  through a diffuse medium of density  $\rho_w$  is  $mdv_c/dt = \rho_w(r)v_c^2 A - m_c g(r)$ . Assuming that the gas is at terminal velocity will give an upper limit to  $\rho_w(r)$ . In this case  $dv_c/dt = 0$  and  $v_t = \sqrt{N_{\text{HI}} \cdot (GM/r^2) / \rho_w(r)}$ , therefore a pure gas cloud with column density  $N_{\text{HI}} = 10^{20} \text{ cm}^{-2}$ , at distances of 10 kpc and 100 kpc moving at  $v_t = 300 \text{ km/s}$  constrains the local IGM  $n_w(10 \text{ kpc}) < 3 \times 10^{-3} \text{ cm}^{-3}$  and  $n_w(100 \text{ kpc}) < 3 \times 10^{-4} \text{ cm}^{-3}$  (for pure gas clouds).

The amount of gas stripped from a dark matter dominated HVC can be estimated using the analytic approach described in Gunn & Gott (1972). The gaseous component will be stripped when the ram pressure of the environment is larger than the gravitational restoration force,  $\rho_w v_w^2 = (\partial\phi_{\text{DM}}/\partial r)\sigma$  where  $\sigma$  is the surface density. This is plotted in Figure 1 for our fiducial dark matter dominated HVC and predicts that it will survive intact for halo densities  $n_w < 10^{-5} \text{ cm}^{-3}$  but would be completely stripped if  $n_w$  is an order of magnitude larger than this.

Figure 1 also shows the results for gas clouds embedded within a cuspy density profile with  $\rho(r) \propto r^{-1}$ . The steeper potential can retain gas more easily and may explain why tiny dwarf galaxies such as Fornax can hold on to gas and form new stars at its center.

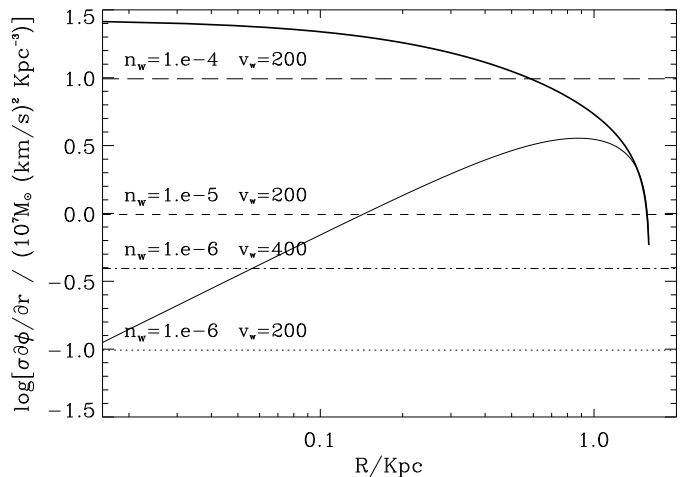


FIG. 1.— The restoration force at different radii within a dark matter dominated HVC. The thin solid curve is for dark matter halos with constant density core with radius 1 kpc and the thick curve shows the behaviour of a density profile with a central cusp  $\rho(r) \propto r^{-1}$ . The far right location where the horizontal lines intersect the restoration force indicates the stripping radius beyond which all the gas will be removed.

### 4. RESULTS

The simulations have been tackled as pure hydro-dynamical processes. The HI is described by a perfect fluid with equation of state  $p = (\gamma - 1)\rho\epsilon$  where  $\rho$  is the density,  $\epsilon$  the specific internal energy, and the adiabatic exponent  $\gamma = 5/3$ . The pure gas HVCs are constructed to be in pressure equilibrium with the external hot medium, whereas the dark matter dominated clouds have an additional potential field that maintains their dynamical equilibrium. In order to integrate the hydro-dynamic equations describing the evolution of HVCs moving through an ionised medium we have used the high-resolution shock-capturing method described in Quilis, Ibáñez and Sáez (1996). This code was specially designed for an accurate treatment of fluid dynamical processes, and is extremely good at dealing with shocks, strong discontinuities, turbulent regions and low density regimes. A specially adapted version for the HVC simulations has been developed. We employ a fixed grid with ratio of sides 2:1:1 and a wind blowing down the long axis. The timestep is set by the minimum Courant condition in the simulation volume which typically sets several hundred steps per crossing time.

We ran a grid of simulations, varying the density and temperature of the external medium from  $10^{-3}$  to  $10^{-6} \text{ cm}^{-3}$  and  $10^6 - 10^4 \text{ K}$  respectively, and cloud velocities between 170 km/s and 400 km/s in order to be conservative. Most of our simulations were run without allowing radiative cooling, although a test run with cooling switched on showed no difference in the response of the HVC to the wind. Our model HVCs are simplistic since they have no internal structure, however we do not expect that this would greatly influence our conclusions.

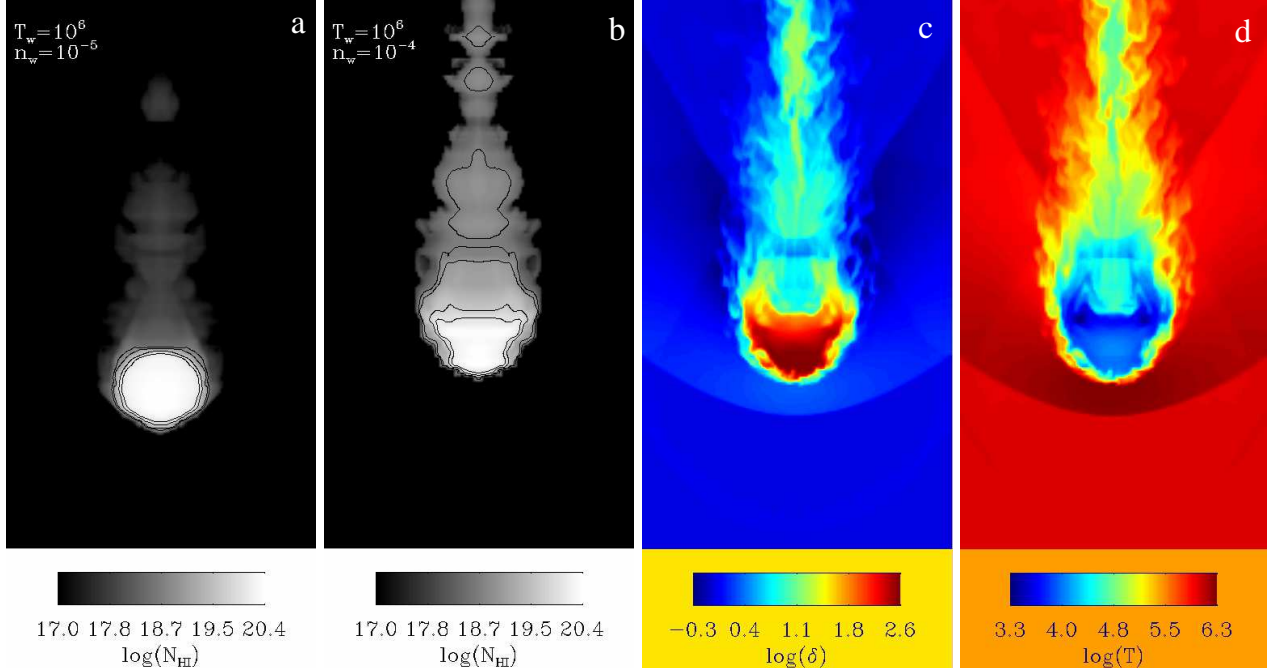


FIG. 2.— The column density for the dark matter dominated HVC after 300 Myrs of evolution in a wind of velocity 200 km/s, (a) density  $10^{-5} \text{ cm}^{-3}$  and (b) density  $10^{-4} \text{ cm}^{-3}$ . The contours correspond to column densities 5, 10.0, 50.0,  $100.0 \times 10^{18} \text{ cm}^{-2}$ . Panels (c) and (d) show the physical density ( $\delta = \rho/\rho_w$ ) and temperature within a central slice through the HVC in panel (b).

#### 4.1. I. Dark matter dominated clouds

Figure 2 shows snapshots of the dark matter dominated HVC after  $3 \times 10^8$  years which is approximately 20 crossing times ( $t_{cr} \sim 2R/v_w$ ) at a wind velocity  $v_w = 200$  km/s. The physical size of the box is  $12 \text{ kpc} \times 12 \text{ kpc} \times 24 \text{ kpc}$ , and the number of cells used  $128 \times 128 \times 256$ , giving a nominal numerical resolution of 90 pc. We ran several test simulations with  $256 \times 256 \times 512$  cells and found no difference with the lower resolutions runs. The grey scale shows the projected surface density of neutral gas and we plot column density contours of cold HI. We define a tail as visible if it has column density higher than  $10^{19} \text{ cm}^{-2}$ . For wind densities  $\leq 2 \times 10^{-5} \text{ cm}^{-3}$  we find no visible tails, although very weak features with  $N_{HI} \sim 10^{18} \text{ cm}^{-2}$  are present.

Panel (b) of Figure 2 shows the same dark matter dominated HVC moving through a medium an order of magnitude denser. Although this may be unrealistic for a Galactic halo component, it does give rise to visible tails of gas. All of the neutral gas has been pushed away from the dark matter potential, as expected from the application of the Gunn and Gott stripping criteria. This material will eventually be completely stripped away and evaporate within the hot component.

In all cases that we simulate we find a similar behaviour. A weak bow shock is visible in front of the cloud that penetrates the IGM and increases its local temperature. The neutral gas at the front edge of the HVC is compressed and heated, whilst a region of low pressure is created immediately behind the cloud. Panels (c) and (d) of Figure 2 shows the rich structure and detail that can be captured with our code. If the wind is not strong enough to cause ram-pressure stripping, viscous/turbulent stripping will continue to remove gas, however, the timescale for this process is fairly long, hence the tails can be quite weak.

#### 4.2. II: Pure gas clouds

Figure 3 shows the evolution of the pure gas clouds. In each case, the physical size of the box is  $180 \text{ pc} \times 180 \text{ pc} \times 360 \text{ pc}$  the number of grid cells used is  $128 \times 128 \times 256$ , giving a numerical resolution of 3 pc. The evolution and features are similar as the dark matter dominated clouds; when the wind is dense enough then visible tails of stripped HI are created.

If the initial column density is too low, the pure gas clouds are compressed at the leading edges and the velocity of the entire cloud decreases as it moves towards its terminal velocity. The main difference between the HVCs in Figure 3(a) and 3(d) are their initial gas densities, which is an order of magnitude higher in Figure 3(d). The IGM density and velocities are the same, but the denser HVC shows visible tails whereas the tails in Figure 3(a) are below  $10^{19} \text{ cm}^{-2}$  and would not be observable.

The mass ratio of gas in the head and tails is typically around 10:1. This result appears very robust regardless of the parameters used in the simulation and is lower than the 3:1 ratio quoted by Brüns et al. (2000). The characteristic lifetimes of the pure gas clouds are quite short and once they enter a diffuse environment that is sufficiently dense to create visible tails, they are rapidly destroyed on a timescale of  $\approx 10^7$  Myrs. Therefore the high fraction of observed clouds with tails suggests that we are observing them soon after they are impacting into a region of high density gas. The tails trail directly behind the motion of the clouds therefore we might expect an alignment effect as the clouds fall directly onto the disk.

### 5. SUMMARY

We have performed hydro-dynamical simulations of HVCs moving through a diffuse medium in an attempt to explain observations of head-tail structures and compres-

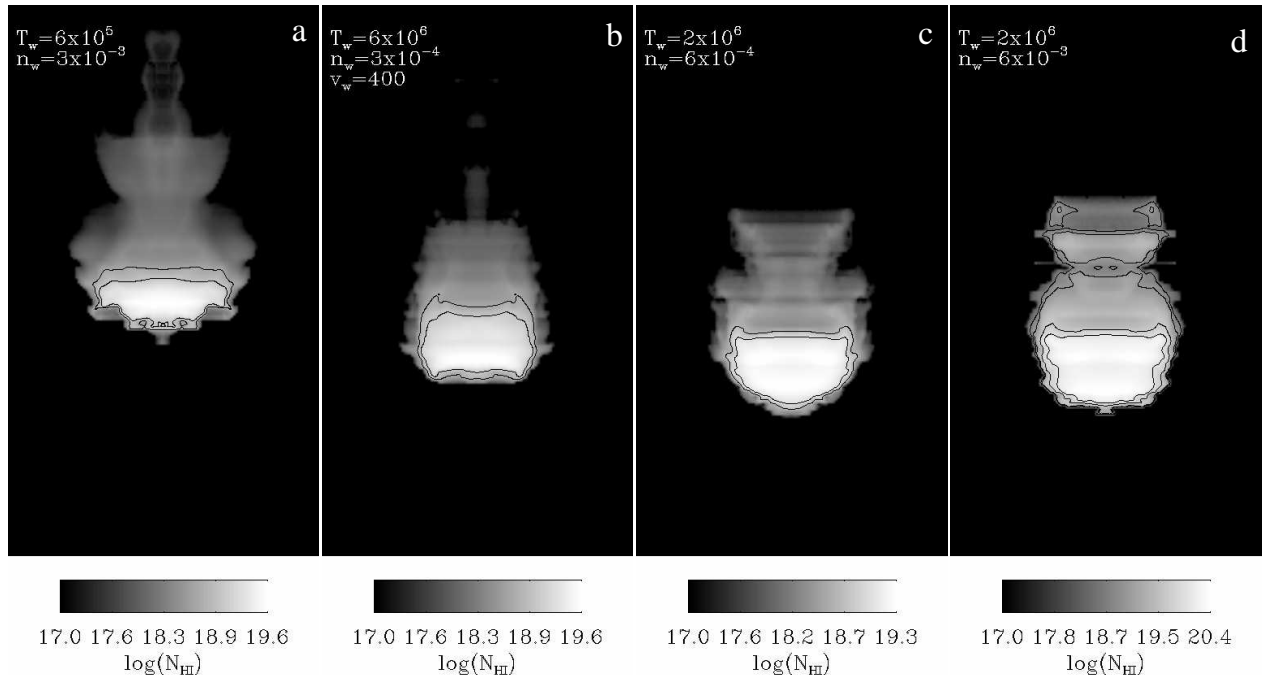


FIG. 3.— Column density maps ( $N_{HI}$ ) for several of the pure gas HVCs after 3 Myrs of evolution. The temperature and density of the external medium are indicated in each panel, and in each case the wind velocity is 200 km/s except panel (b) which is 400 km/s. The initial peak column density in HVCs (a)-(c) is  $2 \times 10^{19} \text{ cm}^{-2}$  whereas model (d) was increased to  $2 \times 10^{20} \text{ cm}^{-2}$ . The contours correspond to column densities 5, 10.0, 50.0,  $100.0 \times 10^{18} \text{ cm}^{-2}$ .

sion fronts. We find that these features are reproduced in either pure gas clouds or gas embedded within a dark matter halo, as long as the wind density is higher than  $10^{-4} \text{ cm}^{-3}$ . This is supported by a simple application of Gunn & Gott's (1972) stripping criteria.

A variety of direct and indirect observations suggest that the density of gas in the outer halo is  $n_w(50\text{kpc}) \lesssim 5 \times 10^{-5} \text{ cm}^{-3}$ . Although observational constraints on the halo gas density at 100–400 kpc are highly uncertain, our naive expectation is that it should decrease at larger radii. The ionised gas close to the Galactic disk can reach much higher densities,  $10^{-3} \text{ cm}^{-3}$ , therefore a Galactic fountain mechanism can reproduce these observations. If the halo gas density increases between 50 and 300 kpc by a factor of two then the observed head-tail structures could also be associated with infalling extra-galactic dark matter dominated clouds.

The lifetime of the neutral tails in our simulations is  $\approx 10^9$  years after which time the column density drops below the observational threshold. Since the observations

suggest that approximately 20% of HVCs show evidence of tails or compression fronts, a timing problem may exist since we must be witnessing the destruction of a large fraction of the HVC population at the current epoch. The Galactic fountain can circumvent this problem since clouds are continuously created and destroyed. The high fraction of clouds with signs of interaction is expected since clouds are only visible as they condense and fall back onto the disk at which point they are susceptible to stripping.

Our simulations show that all HVCs should show tails of stripped gas at lower column densities  $\lesssim 10^{18} \text{ cm}^{-2}$  which may be detectable with higher resolution observations. One may also detect  $H_\alpha$  emission from the secondary shocks that heat the front of the cloud.

**Acknowledgments** We would like to thank Sergio Gelato, Mary Putman and Leo Blitz for useful discussions. VQ is a Marie Curie Fellow (grant HPMF-CT-1999-00052), BM is supported by the Royal Society. Simulations were carried out as part of the Virgo consortium on COSMOS an Origin 2000.

## REFERENCES

- Benjamin, R.A. & Danly, L. 1997, ApJ, 481, 764  
 Benson, A.J., Bower, R.G., Frenk, C.S., & White, S.D.M. 2000, MNRAS, 314, 557  
 Bland-Hawthorn, J. & Maloney, P.R. 1999, ApJLett., 510, L33  
 Blitz, L., Spiegel, D.N., Teuben, P.J., Hartmann, D., & Burton, W.B., 1999, ApJ, 514, 818  
 Blitz, L., & Robishaw, T., 2000, ApJ, 541, 675  
 Braun, R., & Burton, W.B., 1999, A&A, 341, 437  
 Braun, R., & Burton, W.B., 2000, A&A, 354, 853  
 Bregman, J.N., & Houck, J.C. 1997, ApJ, 485, 159  
 Brüns, C., Kerp, J., Kalberla, P.M.W., & Mebold, U., 2000, A&A, 357, 120  
 Brüns, C., Kerp, J., & Pagels, A., 2001, A&ALet. accepted, astro-ph/0103119  
 Ehle, M., Pietsch, W., Beck, R., & Klein, U. 1998, AA, 329, 39  
 Gibson, B.K., Giroux, M.L., Stocke, J.T. & Shull, M. 2001, ASP conference series, eds. J.E. Hibbard, M.P. Rupen & J.H. van Gorkom  
 Gunn, J.E., & Gott, J.R., 1972, ApJ, 176, 1  
 Klypin, A., Kravtsov, A.V., Valenzuela, O., & Prada, F. 1999, ApJ, 522, 8  
 Moore, B. & Davis, M., 1994, MNRAS, 270, 209  
 Moore, B., Ghigna, S., Governato, F., Lake, G., Quinn, T., Stadel, J., & Tozzi, P. 1999, ApJLett, 524, L19  
 Muller, C.A., Oort, J.H., & Raimond, E., 1963, C.R.Acad.Sci.Paris, 257, 1661  
 Murali, C., 2000, A  
 Murray, S.D., White, S.D.M., Blondin, J.M., & Lin, D.N.C., 1993, ApJ, 407, 588  
 Quilis, V., Ibáñez, J.M<sup>a</sup>, & Sáez, D., 1996, ApJ, 469, 11

Snowden, S. L. et al., 1997, ApJ, 485, 125

Wakker, B.P., & van Woerden, H., 1991, A&A, 250, 509

Wolfire, M.G., McKee, C.F., Hollenbach, D., & Tielens A.G.G.M.,  
1995, ApJ, 453, 673